State-Variable-Based Transient Analysis Using Convolution

Carlos E. Christoffersen, *Student Member, IEEE,* Mete Ozkar, *Student Member, IEEE,* Michael B. Steer, *Fellow, IEEE,* Michael G. Case, *Senior Member, IEEE,* and Mark Rodwell, *Member, IEEE*

Abstract—A state-variable-based approach to the impulse response and convolution analysis of distributed microwave circuits is developed. The state-variable approach minimizes computation time and memory requirements. It allows the use of parameterized nonlinear device models, thus improving robustness. Soliton generation on a nonlinear transmission line is considered as an example.

Index Terms— Circuit simulation, circuit transient analysis, convolution, nonlinear circuits, solitons, state variables.

I. INTRODUCTION

TRANSIENT analysis of distributed microwave circuits is complicated by the inability of frequency-independent primitives (such as resistors, inductors, and capacitors) to model distributed circuits. More generally, the linear part of a microwave circuit is described in the frequency domain by network parameters, especially where numerical field analysis is used to model a spatially distributed structure. Inverse Fourier transformation of these network parameters yields the impulse response of the linear circuit. This has been used with convolution to achieve transient analysis of distributed circuits [1]–[4].

The major drawback of convolution analysis has been the large time and memory requirements that result from recording and convolving the nodal voltages of the nonlinear elements. The situation worsens because of convergence considerations that require small time steps. This paper develops a convolution-based transient analysis, which uses state variables instead of node voltages to capture the nonlinear response. This has two desirable effects. First, the number of state variables required is less than the number of nodes of the nonlinear elements and, thus, fewer quantities need to be recorded and convolved. Second, parameterized device models

can be used, as the nonlinearity is not restricted to the form of current as a nonlinear function of voltage. Parameterized device models result in stable transient analysis for larger time steps and, thus, less discretized time history is required. Also, with improved stability, constant time steps can be used, further improving the robustness of the convolution.

A nonlinear transmission line (NLTL) is used here and it is regarded by many in the field as an extreme test of the performance of transient and steady-state simulators. More generally, the work is directed at the transient simulation of distributed systems with tightly coupled circuit-field interactions.

II. BACKGROUND

Distributed linear microwave circuits are described by frequency-dependent network parameters and only a few methods are available to accommodate these circuits in transient simulation. These methods include impulse response and convolution (IRC), asymptotic waveform evaluation (AWE), and Laplace inversion.

A. IRC

One of the first implementations of IRC to distributed microwave circuits was performed in 1987 by Djordjevic and Sarkar [5]. Since that time, there have been several efforts to reduce the significant aliasing errors that result from the inverse fast Fourier transform (I-FFT) operation.

Minimization of aliasing in the I-FFT requires that the imaginary part of the frequency response be zero at the maximum frequency. Low-pass filtering has been used to achieve this [6]. The introduction of a small time delay also achieves this result with presumably less distortion [4]. Insertion of an augmentation network in the linear network at the interface with the nonlinear network achieves the same result for special types of circuits [1]. The effect of the augmentation network is compensated in the nonlinear iteration scheme. It is also important to limit the length of the impulse response to reduce memory requirements, and the resistive augmentation achieves this result [1]. Augmentation is also effectively achieved using *s*-parameters [7], where the reference impedance effectively dampens multiple reflections.

Distributed networks are characterized partly by reflections so that an impulse response tends to have regions of low value between regions of rapid change. In this case, thresholding greatly reduces the number of impulse-response discretizations that need to be retained [1]. In high-speed digital interconnect

circuitry, this can reduce the number of significant impulse responses by a factor of 10–100, depending on the desired accuracy [1].

Convolution, as generally practiced, uses a rectangular integration scheme (essentially an impulse response is treated as being constant in a time-step interval). Stenius *et al.* [8] developed a trapezoidal form of the convolution integration, which could possibly have superior convergence properties than the previous block integration.

B. AWE

The frequency-dependent network parameters can be modeled using frequency-independent primitives (resistors, inductors, and capacitors) if a rational polynomial transfer function is fitted to the network parameters. In practice, this procedure results in an impossibly large circuit. The AWE method addresses this problem by reducing the dimension of the rational polynomial while minimizing distortion [9], [11]. This method works well for interconnects in digital systems and lower frequency microwave circuits [12], [13]. However, higher frequency circuits can only be modeled approximately using AWE due to the infinite number of poles and zeros of such a circuit.

Most of the AWE methods use the Padé approximation and this and other approximations used can have stability problems [9].

Recent work has extended this technique to more general distributed circuits [10].

C. Numerical Inversion of Laplace Transform Technique

This technique does not have aliasing problems since it does not assume that the function is periodic. The inverse transform exists for both periodic and nonperiodic functions. There is no causality problem for double-sided Laplace transforms either. Unlike FFT methods, the desired part of the response can be achieved without doing tedious and unnecessary calculations for the other parts of the response. Laplace techniques suffer from the series approximations and the nonlinear iterations involved. The advantages and limitations of the inverse Laplace methods are discussed in detail in [14].

III. FORMULATION OF THE TRANSIENT ANALYSIS

As it is now conventional for distributed microwave circuits, the circuit is partitioned into linear and nonlinear subcircuits [15]. The core of the method presented here is that state variables are used to describe the nonlinear dependence in the nonlinear subcircuit. This enables more flexibility in writing the nonlinear element models so that better convergence might be achieved [18].

The linear subcircuit is characterized in the frequency domain and the other part, which includes the nonlinear devices, is treated in the time domain. From [16], the vector of voltages $\mathbf{V}_L$ in the frequency domain calculated at the interface to the linear network is

$$\mathbf{V}_L(\mathbf{X}, f) = \mathbf{S}_{SV}(f) + \mathbf{M}_{SV}(f)\mathbf{I}_{NL}(\mathbf{X}, f) \qquad (1)$$

where $\mathbf{X}$ is the state variable vector, $\mathbf{M}_{SV}$ is the state variable impedance matrix, and $\mathbf{I}_{NL}$ is the vector of currents flowing into the linear network at the interface of the linear/nonlinear network. Since the independent sources are more easily handled in the time domain for this kind of analysis, the source vector $\mathbf{S}_{sv}(f)$ can be assumed to be zero and the sources are considered together with the nonlinear devices. Expanding the matrix multiplication, each element of the voltage vector $\mathbf{V}_L(\mathbf{X}, f)$ can be written as

$$V_{L_i} = \sum_{j=1}^{n_S} M_{i,j}(f) I_{NL,j}. \qquad (2)$$

Rewriting one term of this equation in the time domain and replacing the multiplications with the convolution operation leads to

$$v_{L_{i,j}}(t) = m_{i,j}(t) * i_{NL_j}(t). \qquad (3)$$

Now, expanding the convolution operation, we get

$$v_{L_{i,j}}(t) = \int_{-\infty}^{t} m_{i,j}(\tau) i_{NL_j}(t - \tau)\, d\tau \qquad (4)$$

where the system is assumed to be causal: $i_{NL_j}(t) = 0$ for $t \leq 0$. Numerical evaluation requires discretization as follows. First, each element of the I-FFT of $\mathbf{M}_{SV}$ has a finite number of components, which is denoted as N_T. Using the trapezoidal integration rule [8] and using $m_{i,j}$ obtained from the I-FFT, we obtain (5). For $n_t < N_T$, the last term is zero since $i_j(0) = 0$. For $n_t \geq N_T$, the last term is also zero since $m_{i,j}(n_t) = 0$

$$v_{Li,j}(\hat{\mathbf{X}}, n_t)$$
$$= \begin{cases} \dfrac{m_{i,j}(0)i_{NL}(\hat{\mathbf{X}}, n_t)}{2} + \displaystyle\sum_{n_\tau=1}^{n_t-1} m_{i,j}(n_\tau) i_j(n_t - n_\tau), \\ \qquad\qquad\qquad\qquad\qquad\qquad\quad \text{if } n_t < N_T \\ \dfrac{m_{i,j}(0)i_{NL_j}(\hat{\mathbf{X}}, n_t)}{2} + \displaystyle\sum_{n_\tau=1}^{N_T} m_{i,j}(n_\tau) i_j(n_t - n_\tau), \\ \qquad\qquad\qquad\qquad\qquad\qquad\quad \text{if } n_t \geq N_T. \end{cases}$$
$$(5)$$

Note that in all but one of the convolution sum terms, $i_{NL} = i_L = i$; thus, most of the convolution sum can be performed before beginning the iterations to solve the nonlinear system of equations. The following error function is solved at each time step

$$F_i(\hat{\mathbf{X}}) = V_{L_i}(\hat{\mathbf{X}}) - V_{NL_i}(\hat{\mathbf{X}}) \qquad (6)$$

and, in vector form, the complete system is

$$\mathbf{F}(\hat{\mathbf{X}}) = \begin{bmatrix} \displaystyle\sum_{j=1}^{n_s} v_{L_{1,j}}(\hat{\mathbf{X}}, n_t) - v_{NL_1}(\hat{\mathbf{X}}, n_t) \\ \displaystyle\sum_{j=1}^{n_s} v_{L_{2,j}}(\hat{\mathbf{X}}, n_t) - v_{NL_2}(\hat{\mathbf{X}}, n_t) \\ \vdots \\ \displaystyle\sum_{j=1}^{n_s} v_{L_{n_s,j}}(\hat{\mathbf{X}}, n_t) - v_{NL_{n_s}}(\hat{\mathbf{X}}, n_t) \end{bmatrix}. \qquad (7)$$

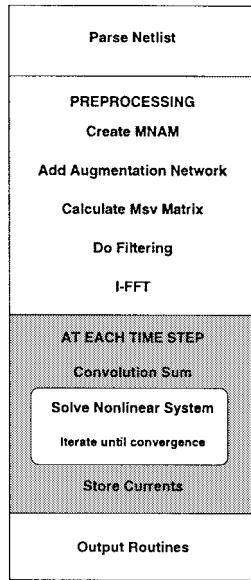The error function in (7) is solved for each time step.

Fig. 1.   Flow diagram of the analysis code.

Fig. 2.   Augmentation and compensation network.

IV. IMPLEMENTATION

The formulation developed above resulted in a standard nonlinear problem that can be solved using the Newton method or quasi-Newton method. As the error function changes only slightly from time step to time step, efficient iterative matrix solve schemes can be used, as a very good preconditioner is available from the previous time step. The general flow of the analysis is shown in Fig. 1 and was implemented in the Transim program.

A. Modified Nodal Admittance Matrix (MNAM)

Computation begins with the formulation and solution of a frequency-domain MNAM of the linear subcircuit. The MNAM routines are based on the sparse matrix package Sparse 1.3.[1] This is a flexible package of subroutines written in C that quickly and accurately solve large sparse systems of linear equations. It also provides utilities such as MNAM reordering and other utilities suited to circuit analysis. At each frequency, the state variable impedance matrix $\mathbf{M}_{SV}$ is calculated from the lower–upper (LU) triangular decomposed MNAM [16].

B. Impulse-Response Determination

The impulse response is obtained using the inverse real Fourier transformation of each element of $\mathbf{M}_{SV}$. The transform requires special characteristics of the frequency-domain variables at high frequencies so that aliasing is minimized. Problems occur with ideal inductors and capacitors, as the matrix elements can go to infinity. This can be corrected by cascading a resistive augmentation circuit with the linear circuit and, thus, ensure finite parameters [1], [17]. The use of scattering parameters achieves similar resistive augmentation [7]. Being resistive, the effect of the augmentation network

can be removed in transient simulation, as the resistors are unaffected by the Fourier transformation. The current work uses the resistive augmentation network shown in Fig. 2. The advantage of this topology is that no extra nodes are added to the circuit and the size of the MNAM is not changed. The augmentation network provides a better matrix conditioning for the I-FFT operation at the expense of increased error due to finite numerical accuracy. Ideally, the effect of the augmentation would be exactly compensated. The resistive augmentation network also serves to limit the extent of the impulse response as energy is absorbed and multiple reflections are damped. Again, note this effect is fully compensated.

Before converting the frequency domain $\mathbf{M}_{SV}$ (impedance-like) matrix to the time domain, the imaginary part of the frequency response needs to be band limited so that the function has a periodic (or circular) frequency response. This significantly reduces the aliasing errors in the I-FFT operation.

In Transim, frequency response limiting is implemented by filtering the last part of the frequency spectrum of each matrix element so the imaginary part goes to zero and the real part goes to the dc value. In this way, the frequency response is periodic. This is in contrast to low-pass filtering [1], which zeroes the high-frequency response and introducing additional time delay to take the imaginary response to zero [2]. The filtering factor k_i is

$$k_i = \left(\frac{n-i}{n-i_0} \right)^2 \tag{8}$$

where n is the number of discrete frequencies, i is the frequency index, and i_0 is the frequency index at which filtering starts. For all i greater than i_0, the filtering operation on each state variable impedance matrix entry is

$$\Re\{m_i\} = k_i \times \Re\{m_i\} + (1 - k_i) \times m_0 \tag{9}$$

$$\Im\{m_i\} = k_i \times \Im\{m_i\}. \tag{10}$$

The amount of filtering is an analysis option since, in some cases, it is not necessary. By default, only the last 3% of the

[1] K. S. Kundert and A. Sangiovanni-Vincentelli, "Sparse User's Guide: A sparse linear equation solver," Version 1.3a, Dept. Elect. Eng. Comput. Sci., Univ. California at Berkeley, Berkeley, CA 94720, 1988.
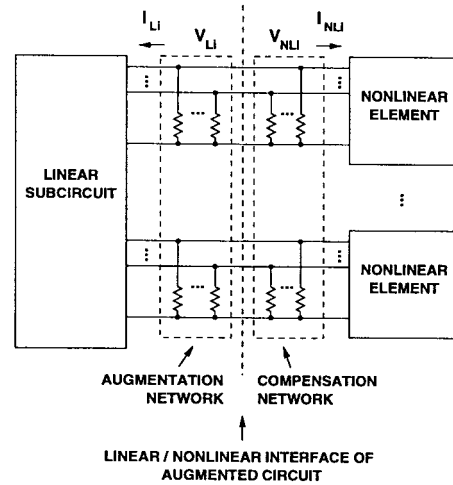
spectrum is filtered to achieve an acceptable alias reduction. The effect on causality remains to be determined. If this is not done, the correct impulse response is not assured as the continuity condition is inherent in the I-FFT (or FFT) operation.

Causality imposes special considerations for the response obtained from the I-FFT operation. A discontinuity of the impulse response generally occurs at $t = 0$, as the negative time response must be zero [8]. In this situation, the I-FFT operation yields a value which is the average of the one-sided limits of the function at that point; i.e., the value calculated at $t = 0$ is one-half of the value at $t = 0^+$. However, the upper side limit (at $t = 0^+$) is required in numerical integration and, thus, the value of the I-FFT calculated time response must be multiplied by two to obtain the required impulse response. Note that in (5), the first point of the impulse is divided by two; thus, the multiplication can actually be saved.

Fourier transformation is implemented using a real I-FFT algorithm from the FFTW library.[2] This algorithm requires only the positive frequency samples since the negative frequency samples are the complex conjugate of the corresponding positive frequencies. The FFTW library is a comprehensive collection of C routines for computing the discrete Fourier transform in one or more dimensions of both real and complex data and of arbitrary input size.

C. Parameterized Nonlinear Models

Let the nonlinear subnetwork be described by the following generalized parametric equations [18]:

$$\mathbf{v}_{NL}(t) = u\left[\mathbf{x}(t), \frac{d\mathbf{x}}{dt}, \cdots, \frac{d^n\mathbf{x}}{dt^n}, \mathbf{x}_D(t)\right] \quad (11)$$

$$\mathbf{i}_{NL}(t) = w\left[\mathbf{x}(t), \frac{d\mathbf{x}}{dt}, \cdots, \frac{d^n\mathbf{x}}{dt^n}, \mathbf{x}_D(t)\right] \quad (12)$$

where $v_{NL}(t)$, $i_{NL}(t)$ are vectors of voltages and currents at the common ports, $\mathbf{x}(t)$ is a vector of state variables, and $\mathbf{x}_D(t)$ a vector of time-delayed state variables, i.e., $x_{Di}(t) = x_i(t - \tau_i)$. The time delays τ_i may be functions of the state variables. All vectors in (12) have the same size n_d equal to the number of common (device) ports. This kind of representation is convenient from the physical viewpoint, as it is equivalent to a set of implicit integro-differential equations in the port currents and voltages. This allows an effective minimization of the number of subnetwork ports and, what is more important, results in extreme generality in device modeling capabilities.

Here, a parametric diode model for the diode element is presented [18]. The full model includes capacitances and nonlinear resistance, but here, a simple case is shown for didactic purposes. The conventional current equation for the diode is

$$i(t) = I_s\left(\exp(\alpha v(t)) - 1\right) \quad (13)$$

[2] M. Frigo and S. G. Johnson, *FFTW User's Manual*. Cambridge, MA: MIT, 1998.
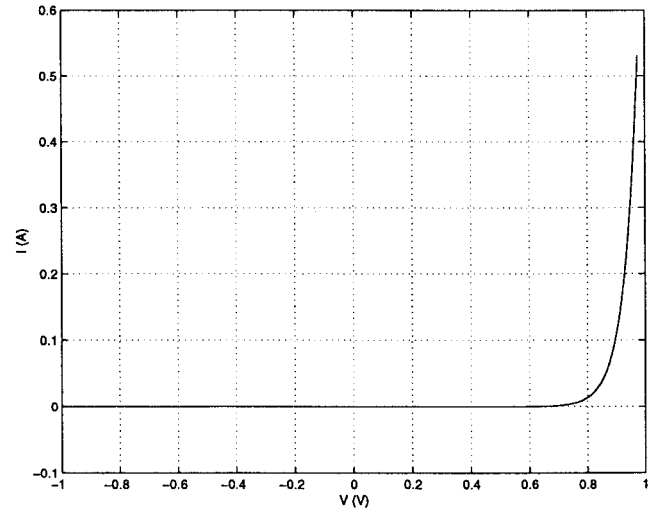

Fig. 3. Relation between v and i in a diode.

and, based on previous work [18], the parametric model is as follows:

$$v(t) = \begin{cases} x(t), & \text{if } x(t) \leq V_1 \\ V_1 + \dfrac{1}{\alpha} \ln(1 + \alpha(x(t) - V_1)), & \text{if } x(t) > V_1 \end{cases} \quad (14)$$

$$i(t) = \begin{cases} I_s(\exp(\alpha x(t)) - 1), & \text{if } x(t) \leq V_1 \\ I_s \exp(\alpha V_1) \\ \quad \cdot (1 + \alpha(x(t) - V_1)) - I_s, & \text{if } x(t) > V_1 \end{cases} \quad (15)$$

where V_1 is some threshold value. The model requires the current, voltage, and derivatives to be continuous at $x = V_1$. This implies that
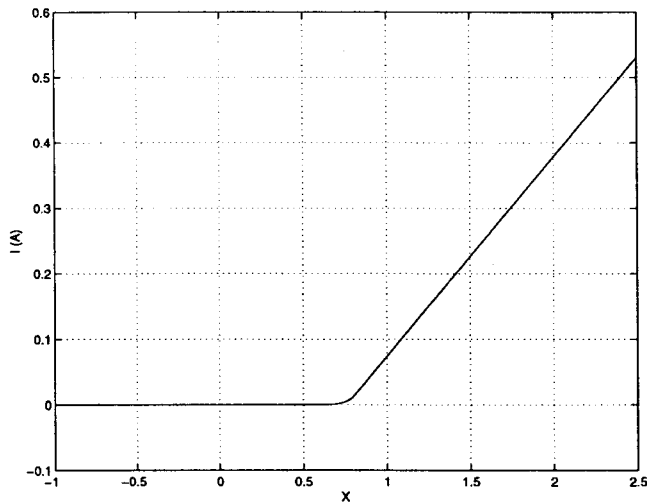
$$V_1 = \frac{\ln(G_1/\alpha I_s)}{\alpha} \quad (16)$$

where G is the slope $\partial i/\partial v$ and is chosen to be $5e8 \cdot I_s$. Note that using this value, V_1 becomes independent of the saturation current. In this way, the maximum value of the exponential function is limited to $5e8$.

The plots of Figs. 3–5 show the improvement in the behavior of the model when using the state variable approach. In a diode, the current has an exponential dependence on voltage. This causes convergence problems when the voltage is updated during nonlinear iteration. At voltages greater than the threshold, small voltage increments can result in large current changes and, hence, changes in the error function. The possibility of large changes is eliminated through the use of parameterization that ensures smooth well behaved current, voltage, and error function variations when the state variable is updated (see Figs. 4 and 5).

D. Convolution

Convolution of the impulse response of the linear circuit with the outputs of the nonlinear elements has been proposed for transient analysis of distributed circuits with [1]–[4], [6], [7], and [19]. The major problem identified with this type of analysis is the rapid growth in computation

Fig. 4. Relation between x and i in a diode.
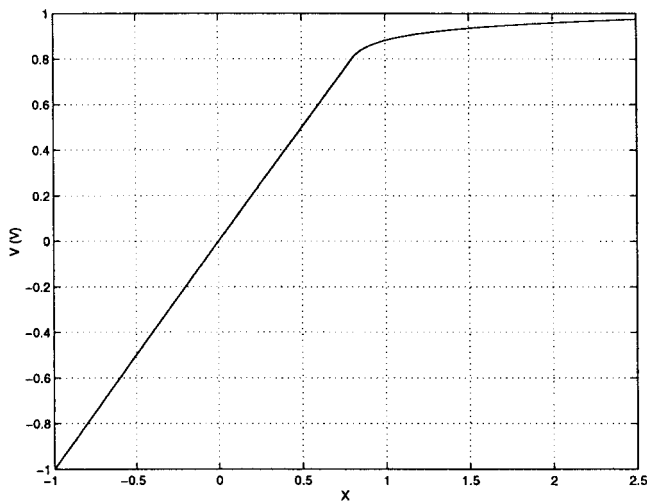
Fig. 5. Relation between x and v in a diode.

and memory requirements. The convolution integral, which becomes a convolution sum in computer implementations, is $O(n_{MAX}^2 n_S^2)$ where n_{MAX} is the length of the impulse response and n_S is the number of state variables. Memory usage is $O(n_{MAX} \times n_S^2)$, principally due to storage of the matrix impulse response. Thus, reducing the number of state variables n_S (i.e., using the minimum number of state variables rather than the voltages at all nodes of the nonlinear network) dramatically reduces memory and compute time. As state variables permit the use of parameterized device models, the stability of the convolution analysis is improved, allowing larger time steps and, thus, reducing n_{MAX}.

E. Nonlinear Equation Solver

The nonlinear system at each time step is solved using the NNES library.[3] It is written in Fortran and provides Newton and quasi-Newton methods and many options, such as the use of analytic Jacobian or forward, backward, or central

[3] R. S. Bain, *NNES User's Manual* (1993). [Online.] Available HTTP: http//www.netlib.org/opt/
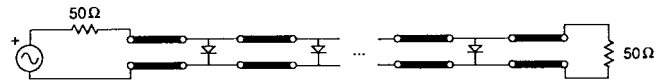

Fig. 6. Model of the NLTL.

differences to approximate it, different quasi-Newton Jacobian updates, and two globally convergent methods. This flexibility permits rapid simulator development. Additionally, it reflects state-of-the-art numerical analysis.

V. SIMULATION OF A NLTL

NLTL's find applications in a variety of high-speed wide-bandwidth systems, including picosecond resolution sampling circuits, laser and switching diode drivers, test waveform generators, and millimeter-wave sources [20]. They have the following three fundamental characteristics:

1) nonlinearity;
2) dispersion;
3) dissipation.

NLTL's consist of coplanar waveguides (CPW's) periodically loaded with reverse-biased Schottky diodes. Diode-based NLTL's used for pulse generation are extremely nonlinear circuits and are being used to test the robustness of circuit simulators. The NLTL considered here was designed with a balance between the nonlinearity of the loaded nonlinear elements and the dispersion of the periodic structure, which results in the formation of a stable soliton [21], [22]. The nonlinearity of NLTL's is principally due to the voltage-dependent capacitance of the diodes, and the dissipation is due to the conductor losses in the CPW's.

In this paper, the NLTL was modeled using generic transmission lines with frequency-dependent loss and Schottky diodes.[4] Skin effect was taken into account in the modeling of the transmission lines. The NLTL model is shown in Fig. 6 and is excited by a 9-GHz sinusoid. The NLTL was designed for a 24-GHz initial Bragg frequency, 225-GHz final Bragg frequency, 0.952 097 tapering rule, and 120-ps total compression. It contains 48 sections of CPW transmission lines and 47 diodes. The drive is a 27-dBm sine wave with −3-V DC bias.

VI. RESULTS AND DISCUSSION

Fig. 7 shows the calculated transient response of the soliton line, including frequency-dependent (skin effect) loss of the transmission lines. The simulation time was 8 h on an Ultra-SPARC 1 workstation, clocked at 143 MHz. The number of frequencies used to obtain the impulse response was 4096 and the maximum frequency was 2700 GHz, which corresponds to a time step of 0.185 ps. The value of the compensation resistor was 140 Ω. The comparison among the measured output voltage across the load [20] and transient and harmonic-balance simulation (also using Transim) is shown in Fig. 8. The harmonic-balance analysis used the state-variable approach described in [16]. The convergence rate was increased

[4] "Microwave Harmonica Elements Library," Compact Software, Paterson, NJ, 1994.
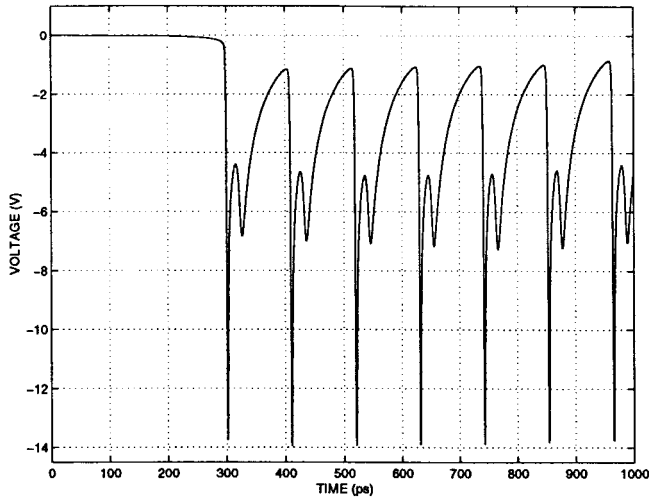
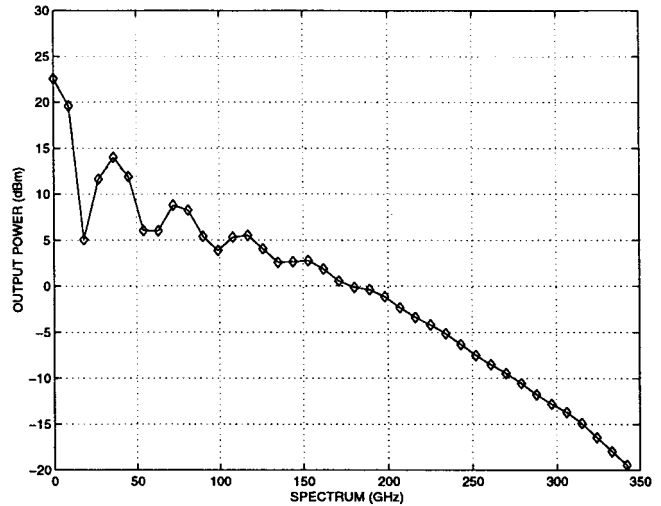Fig. 7. Complete transient response for the soliton line.

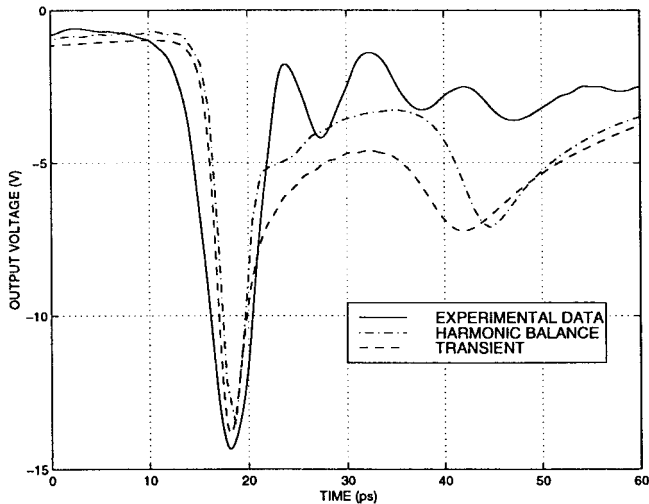Fig. 9. Magnitude of the harmonics of the output power.

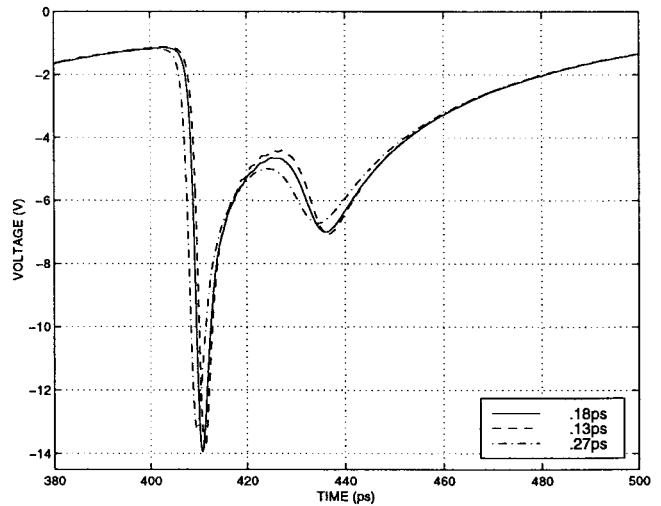Fig. 8. Comparison between experimental data and simulations.

Fig. 10. Comparison between simulations using different time steps.

and the number of harmonics was reduced using the filtering technique described in [23], starting at harmonic number 30. The total number of frequencies was 40, and the simulation time was 30 h on the same computer. The harmonic content of the output is shown in Fig. 9. The prediction of the main soliton amplitude is correct, although the impulse width is slightly smaller in the simulations. Note that the secondary soliton predicted by the simulations is not observed in the measurements. This is probably due to neglecting higher order parasitic effects of the interconnections. In both simulations, a parasitic inductance of 21.8 pH modeled the connection between each diode and the CPW line. Without adding complexity, this inductor was incorporated in the nonlinear diode model. This is only possible with state variables, and results in a better conditioned transient analysis.

The transient analysis gives slightly different responses depending on the size of the time step, as shown in Fig. 10. Smaller time step yields a simulation more accurate. Work continues to identify the required time step for a prescribed accuracy. The importance of IRC analysis of distributed microwave circuits, as opposed to conventional SPICE analysis, is that frequency-dependent linear elements can be handled. In
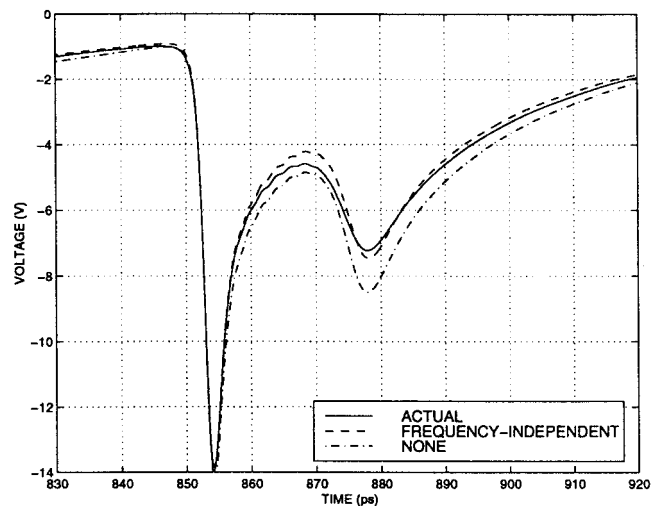

Fig. 11. Comparison between simulations using different attenuation factors for the transmission lines.

Fig. 11, the effect of frequency-dependent transmission-line attenuation, principally due to the skin effect, is compared to frequency-independent attenuation and no attenuation. The

frequency-independent attenuation of the transmission lines is the attenuation at 10 GHz. Frequency-dependent attenuation has only a small effect on the depth and width of the soliton. The importance of modeling is borne out by these results. Rather than focusing on the previously deleterious effect of frequency-dependent loss, better modeling of the parasitics of the NLTL is required to provide a better basis for computer-aided design.

VII. CONCLUSION

The importance of this paper was the development of a state-variable formulation for transient analysis of distributed circuits using the impulse response of the linear subnetwork and convolution. State-variable-based analysis minimizes compute time and memory requirements when the number of linear elements with frequency-dependent loses is greater or about the same as the number of nonlinear elements, but, most importantly, it improves the robustness of the simulation by allowing parameterized nonlinear device models to be used. The transient simulation technique developed here is targeted at the analysis of circuits with tightly coupled circuit and field interactions. Modeling of the electromagnetic environment results in port descriptions without a defined global reference node, rendering the use of nodal voltages problematic [24], [25]. The current implementation of Transim circumvents this problem by the use of local reference nodes.

REFERENCES

[1] M. S. Basel, M. B. Steer, and P. D. Franzon, "Simulation of high speed interconnects using a convolution-based hierarchical packaging simulator," *IEEE Trans. Comp., Packag., Manufact. Technol. B,* vol. 18, pp. 74–82, Feb. 1995.

[2] T. J. Brazil, "A new method for the transient simulation of causal linear systems described in the frequency domain," in *IEEE MTT-S Int. Microwave Symp. Dig.* June 1992, pp. 1485–1488.

[3] P. Perry and T. J. Brazil, "Hilbert-transform-derived relative group delay," *IEEE Trans. Microwave Theory Tech.,* vol. 45, pp. 1214–1225, Aug. 1997.

[4] T. J. Brazil, "Causal convolution—A new method for the transient analysis of linear systems at microwave frequencies," *IEEE Trans. Microwave Theory Tech.,* vol. 43, pp. 315–323, Feb. 1995.

[5] A. R. Djordjevic and T. K. Sarkar, "Analysis of time response of lossy multiconductor transmission line networks," *IEEE Trans. Microwave Theory Tech.,* vol. MTT-35, pp. 898–908, Oct. 1987.

[6] D. Winkelstein, R. Pomerleau, and M. B. Steer, "Transient simulation of complex lossy multiport transmission line networks with nonlinear digital device termination using a circuit simulator," in *Proc. IEEE Southeastcon Conf.,* vol. 3, 1991, pp. 1239–1244.

[7] J. E. Schutt-Aine and R. Mittra, "Nonlinear transient analysis of coupled transmission lines," *IEEE Trans. Circuits Syst.,* vol. 36, pp. 959–967, July 1989.

[8] P. Stenius, P. Heikkilä, and M. Valtonen, "Transient analysis of circuits including frequency-dependent components using transgyrator and convolution," in *Proc. 11th European Conf. Circuit Theory Design,* pt. III, 1993, pp. 1299–1304.

[9] P. K. Chan, "Comments on 'Asymptotic waveform evaluation for timing analysis,'" *IEEE Trans. Computer-Aided Design,* vol. 10, pp. 1078–1079, Aug. 1991.

[10] R. Archar, M. S. Nakhla, and Q.-J. Zhang, "Full-wave analysis of high speed interconnects using complex frequency hopping," *IEEE Trans. Computer-Aided Design,* vol. 17, pp. 997–1010, Oct. 1998.

[11] M. Celik, O. Ocali, M. A. Tan, and A. Atalar, "Pole–zero computation in microwave circuits using multipoint Padé approximation," *IEEE Trans. Circuits Syst.,* vol. 42, pp. 6–13, Jan. 1995.

[12] E. Chiprout and M. Nakhla, "Fast nonlinear waveform estimation for large distributed networks," in *IEEE MTT-S Int. Microwave Symp. Dig.*, vol. 3, June 1992, pp. 1341–1344.

[13] R. J. Trihy and Ronald A. Rohrer, "AWE macromodels for nonlinear circuits," in *Proc. 36th Midwest Circuits Syst. Symp.,* vol. 1, Aug. 1993, pp. 633–636.

[14] R. Griffith and M. S. Nakhla, "Mixed frequency/time domain analysis of nonlinear circuits," *IEEE Trans. Computer Aided Design,* vol. 11, pp. 1032–1043, Aug. 1992.

[15] M. S. Nakhla and J. Vlach, "A piecewise harmonic balance technique for determination of periodic response of nonlinear systems," *IEEE Trans. Circuits Syst.,* vol. CAS-23, pp. 85–91, Feb. 1976.

[16] C. E. Christoffersen, M. B. Steer, and M. A. Summers, "Harmonic balance analysis for systems with circuit-field interactions," in *IEEE Int. Microwave Symp. Dig.,* June 1998, pp. 1131–1134.

[17] M. Ozkar, "Transient analysis of spatially distributed microwave circuits using convolution and state variables," M.S. thesis, Dept. Elect. Comput. Eng., North Carolina State Univ., Raleigh.

[18] V. Rizzoli, A. Lipparini, A. Costanzo, F. Mastri, C. Cecchetti, A. Neri, and D. Masotti, "State-of-the-art harmonic-balance simulation of forced nonlinear microwave circuits by the piecewise technique," *IEEE Trans. Microwave Theory Tech.,* vol. 40, pp. 12–27, Jan. 1992.

[19] C. Gordon, T. Blazeck, and R. Mittra, "Time domain simulation of multiconductor transmission lines with frequency-dependent losses," *IEEE Trans. Computer-Aided Design,* vol. 11, pp. 1372–1387, Nov. 1992.

[20] M. G. Case, "Nonlinear transmission lines for picosecond pulse, impulse and millimeter-wave harmonic generation," Ph.D. dissertation, Dept. Elect. Comput. Eng., Univ. California at Santa Barbara, Santa Barbara, CA, 1993.

[21] M. J. W. Rodwell, M. Kamegawa, R. Yu, M. Case, E. Carman, and K. S. Giboney, "GaAs nonlinear transmission lines for picosecond pulse generation and millimeter-wave sampling," *IEEE Trans. Microwave Theory Tech.,* vol. 39, pp. 1194–1204, July 1991.

[22] H. Shi, C. W. Domier, and N. C. Luhmann, "A monolithic nonlinear transmission line system for the experimental study of lattice solutions," *J. Appl. Phys.,* vol. 4, pp. 2558–2564, Aug. 1995.

[23] A. Brambilla and D. D'Amore, "A filter-based technique for the harmonic balance method," *IEEE Trans. Circuits Syst. I,* vol. 43, pp. 92–98, Feb. 1996.

[24] A. I. Khalil and M. B. Steer, "Circuit theory for spatially distributed microwave circuits," *IEEE Trans. Microwave Theory Tech.,* vol. 46, pp. 1500–1503, Oct. 1998.

[25] C. E. Christoffersen and M. B. Steer, "Implementation of the local reference concept for spatially distributed circuits," *Int. J. RF Microwave Computer-Aided Eng.,* to be published.

Carlos E. Christoffersen (S'91), for photograph and biography, see this issue, p. 838.

Mete Ozkar (S'97) received the B.S. degree in electrical engineering from the Middle East Technical University, Ankara, Turkey, in 1996, the M.S. degree from North Carolina State University, Raleigh, NC, in 1998, and is currently working toward the Ph.D. degree in electrical engineering at the same university.

He is currently a Research Assistant in the Electronics Research Laboratory, Department of Electrical and Computer Engineering, North Carolina State University, where he performs research in the simulation and the development of spatial power-combining systems.

Michael B. Steer (S'76–M'78–SM'90–F'99), for photograph and biography, see this issue, p. 816.
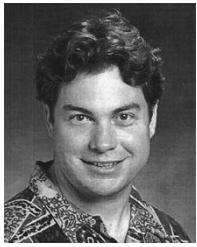
Michael G. Case (S'88–M'91–SM'98) was born in Ventura, CA, in 1966. He received the B.S., M.S., and Ph.D. degrees from the University of California at Santa Barbara, in 1989, 1991, and 1993, respectively.

In 1989, he began research work at he University of California at Santa Barbara, where he studied NLTL's for applications in high-speed waveform shaping and signal detection. Since 1993, he has been with HRL Laboratories, Malibu, CA, where he is currently involved with millimeter-wave device characterization, circuit design, and measurement techniques.

Dr. Case was the recipient of a state fellowship.
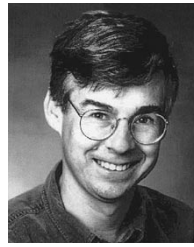
Mark Rodwell (M'89) was born in Altrincham, U.K., in 1960. He received the B.S. degree in electrical engineering from the University of Tennessee, Knoxville, in 1980, and the M.S. and Ph.D. degrees in electrical engineering from Stanford University, Stanford, CA, in 1982 and 1988, respectively.

From 1982 to 1984, he was with AT&T Bell Laboratories, where he developed optical transmission systems. He was a Research Associate at Stanford University from January to September 1988. In September 1988, he joined the Department of Electrical and Computer Engineering, University of California at Santa Barbara, where he is currently a Professor and Director of the Compound Semiconductor Research Laboratories. His current research involves submicrometer scaling of millimeter-wave heterojunction bipolar transistors (HBT's), development of HBT integrated circuits for microwave mixed-signal integrated circuits (IC's), and fiber-optic transmission systems. His group has developed deep submicrometer Schottky-collector resonant-tunnel diodes with terahertz bandwidths, and has developed monolithic submillimeter-wave oscillators with these devices. His group has worked extensively in the area of GaAs Schottky-diode IC's for subpicosecond pulse generation, signal sampling at submillimeter-wave bandwidths, and millimeter-wave instrumentation.

Dr. Rodwell was the recipient of the 1989 National Science Foundation Presidential Young Investigator Award and his work on submillimeter-wave diode IC's was awarded the 1997 IEEE Microwave Prize.